Modelling Hysteresis in the Force Characteristic of the Fluidic Muscles

József Sárosi

Faculty of Engineering University of Szeged, Mars sq. 7, H-6724, Szeged, Hungary, sarosi@mk.u-szeged.hu

Abstract: Pneumatic artificial muscle (PAM) is the newest and most promising type of pneumatic actuators. The force and motion produced by PAMs are linear and unidirectional. Different designs of PAMs have already been developed. Recently Fluidic Muscle manufactured by Festo Company and Shadow Air Muscle manufactured by Shadow Robot Company are the most popular and commercially available. The muscle force as a function of contraction (relative displacement) at constant values of pressure is the most frequently mentioned feature of PAMs. In the force-contraction cycle hysteresis can be observed. This paper presents comparisons between the measured and theoretical data of the hysteresis loop using a six-parameter function. To verify the accuracy of fitting of the function mathematical method of statistics is applied in MS Excel.

Keywords: Fluidic Muscle, Static Model, Hysteresis, Correlation

1 Introduction

The working principle of different pneumatic muscles is well described in [1], [2], [3], [4], [5] and [6]. PAMs have various names in literature: Pneumatic Muscle Actuator, Fluid Actuator, Fluid-Driven Tension Actuator, Axially Contractible Actuator, Tension Actuator, etc. [3], [4], [7].

Most types of PAMs consist of a rubber bladder enclosed within a helical braid that is clamped on both ends. A PAM's energy source is gas, usually air. The muscle will expand radially and contract axially when inflated, while generating high pulling forces along the longitudinal axis. The tensile force depends on the contraction and applied pressure (Fig. 1). This feature is totally different from pneumatic cylinders, because a cylinder develops a force that depends on the applied pressure and piston surface area and the force does not depend on displacement [4]. Typically, the air muscle can contract by about 25 % of its initial length.

In the force-contraction cycle hysteresis can be observed. Chou and Hannaford in [2] report hysteresis to be substantially due to Coulomb friction, which is caused by the contact between the bladder and the shell, between the braided threads and each other and the shape changing of the bladder.

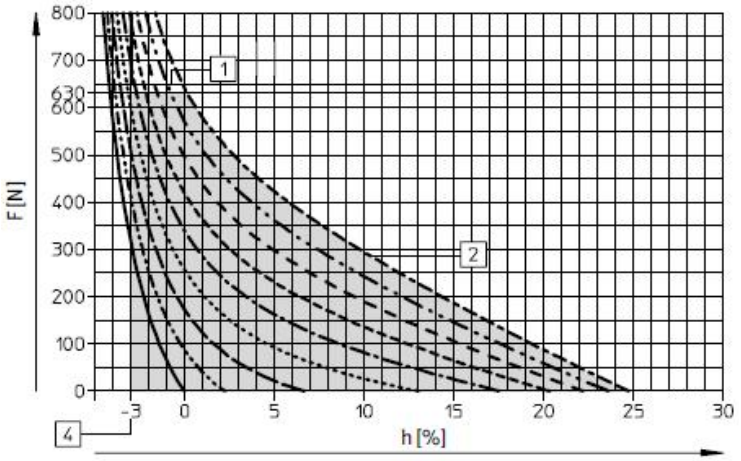

Figure 1
Isobaric force-contraction characteristics of Fluidic Muscle with inner diameter of 10 mm [8]

Where:
1 maximal force,
2 maximal operating pressure,
3 maximal deformation (contraction),
4 maximal pretensioning.

Many researchers have investigated the relationship between the force, length and pressure to find a good theoretical approach for the equation of force produced by pneumatic artificial muscles. Some of them report several static and dynamic models [2], [5], [7], [10], [11], [12], [13]. Our goal was to develop a precise approximation algorithm with minimum number of parameters for the force of different Fluidic Muscles.

The layout of this paper is as follows. Section 2 (Static Force Model of Pneumatic Artificial Muscles) is devoted to illustrate the static models on the basis of professional literature and our new force model. Section 3 (Experimental Results) presents comparison between the measured and theoretical data for the hysteresis loop. Finally, section 4 (Conclusions) gives the investigations we plan.

For this study Fluidic Muscle type DMSP-10-100N-RM-RM (with inner diameter of 10 mm and initial length of 100 mm) produced by Festo Company is selected.

2 Static Force Model of Pneumatic Artificial Muscle

The general behaviour of PAM with regard to shape, contraction and tensile force when inflated depends on the geometry of the inner elastic part and of the braid at rest (Fig. 2), and on the materials used [3]. Typical materials used for the membrane construction are latex and silicone rubber, while nylon is normally used in the fibres. Fig. 3 shows the materials of Fluidic Muscles. The load carrying structure of Fluidic Muscles is embedded helically in its membrane. The membrane is made from chloroprene and the load carrying structure is made from aramid.

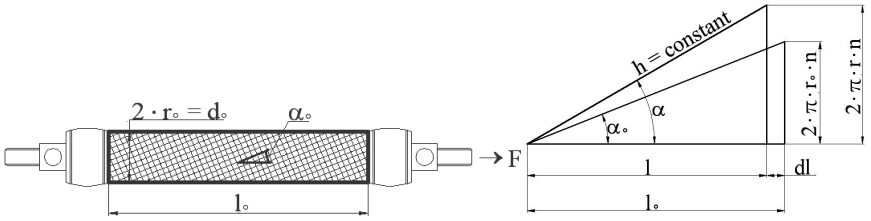

Figure 2
Geometry parameters of PAM

Where:
F the pulling force,
r_0 the initial inner radius of PAM,
l_0 the initial length of PAM,
α_0 the initial angle between the thread and the muscle long axis,
r the inner radius of the PAM when the muscle is contracted,
l the length of the PAM when the muscle is contracted,
α the angle between the thread and the muscle long axis when the muscle is contracted,
h the constant thread length,
n the number of turns of thread.

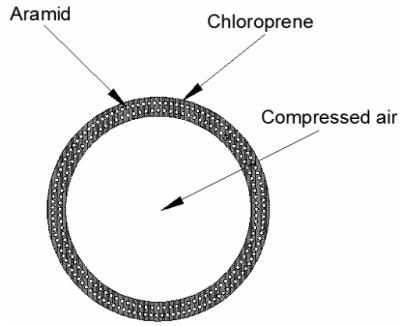

Figure 3
Scheme of Fluidic Muscles

Good description of the general static models of PAMs can be found in [2], [3], [5] and [14]. On the basis of them the force equation is found:

$$F(p,\kappa) = r_0^2 \cdot \pi \cdot p \cdot (a \cdot (1-\kappa)^2 - b) \quad (1)$$

Where: $a = \frac{3}{tg^2\alpha_0}$, $b = \frac{1}{\sin^2\alpha_0}$, $\kappa = \frac{l_0 - l}{l_0}$ and

p the applied pressure,
κ the contraction.

Equation 1 was modified by Tondu and Lopez in [5] and Kerscher et al. in [11] with correction factors ε and μ:

$$F(p,\kappa) = \mu \cdot r_0^2 \cdot \pi \cdot p \cdot (a \cdot (1-\varepsilon \cdot \kappa)^2 - b) \quad (2)$$

Significant differences between the theoretical and experimental results using (1) and (2) have been proved in [14] and [15]. To eliminate the differences new approximation algorithm with six unknown parameters has been introduced for the force generated by Fluidic Muscles:

$$F(p,\kappa) = (a_1 \cdot p + a_2) \cdot \exp^{a_3 \cdot \kappa} + a_4 \cdot \kappa \cdot p + a_5 \cdot p + a_6 \quad (3)$$

Equation 3 can be generally used with high accuracy for different Fluidic Muscles independently from length and diameter under different values of pressure.

The unknown parameters of (3) are found using least squares method with Microsoft Excel Solver.

3 Experimental Results

The analyses were carried out in MS Excel environment. Firstly, tensile force of Fluidic Muscle under a pressure of 600 kPa was determined as shown in Fig. 4.

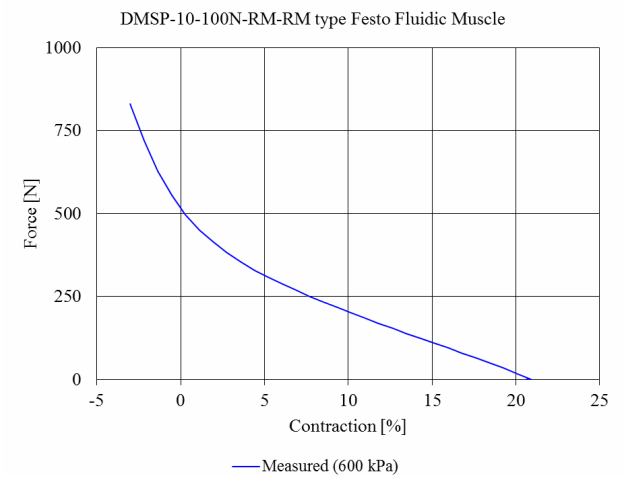

Figure 4
Isobaric force-contraction diagram of Fluidic Muscle under a pressure of 600 kPa

To approximate the measured force generated by Fluidic Muscles type DMSP-10-100N-RM-RM (3) was used. Values of the unknown parameters of (3) are shown in Table 1.

Table 1
Values of unknown parameters of (3) (600 kPa)

Parameters	Values
a_1	-13.57
a_2	215.53
a_3	-0.36
a_4	-3.04
a_5	99.74
a_6	-215.33

Fig. 5 presents the experimental and theoretical results on the same graph. To describe the nature and strength of the relationship between the experimental and calculated results, regression and correlation analysis were used. $R^2 = 0.9999 \rightarrow R = 0.99995$ coefficient approaches the maximum (strongest, R = 1) correlation (Fig. 6).

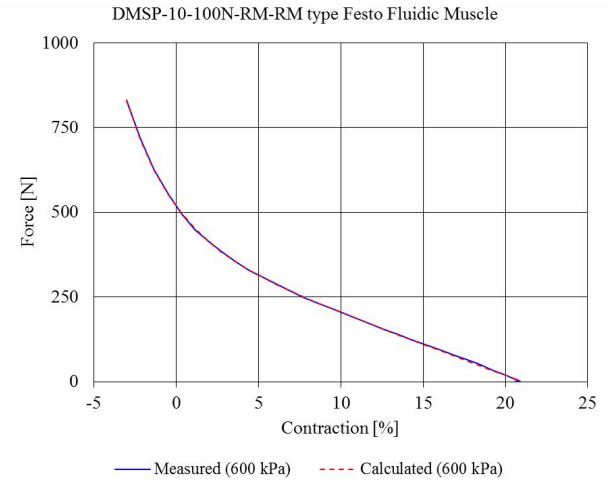

Figure 5
Comparison of measured and calculated force under a pressure of 600 kPa using (3)

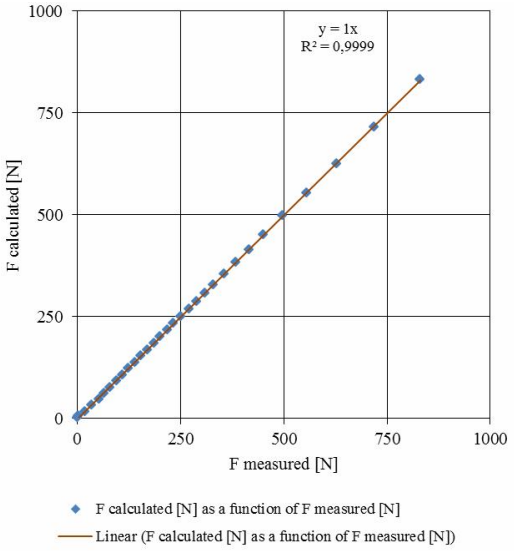

Figure 6
Result of regression and correlation analysis under a pressure of 600 kPa

Secondly, the investigation was repeated under different pressure values (0-600 kPa). The force always drops from its highest value at full muscle length to zero at full inflation and position (Fig. 7).

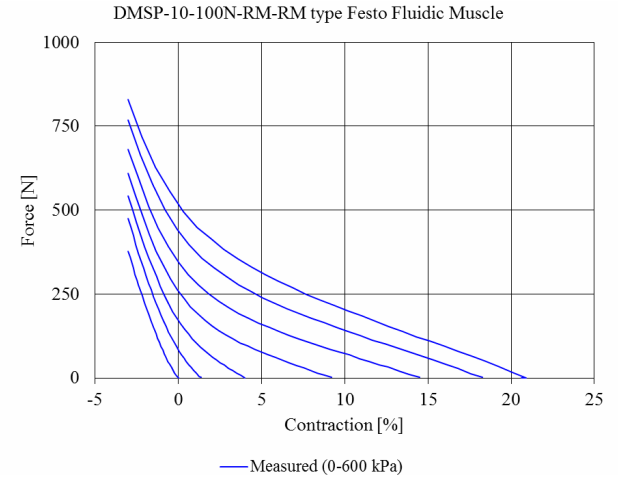

Figure 7
Isobaric force-contraction diagram of Fluidic Muscle under different pressure values (0-600 kPa)

The accurate fitting of (3) can be seen in Fig. 8 and Fig. 9 illustrates the relationship between the measured force and calculated force. The $R^2 = 0.9989 \rightarrow R = 0.9994$ coefficient proves the tight relationship between them, i.e. the correlation coefficient slightly reduced if the pressure is extended to the range of 0-600 kPa. Values of the unknown parameters of (3) are shown in Table 2.

Table 2
Values of unknown parameters of (3) (0-600 kPa)

Parameters	Values
a_1	-13.05
a_2	215.62
a_3	-0.35
a_4	-3.08
a_5	100.49
a_6	-215.22

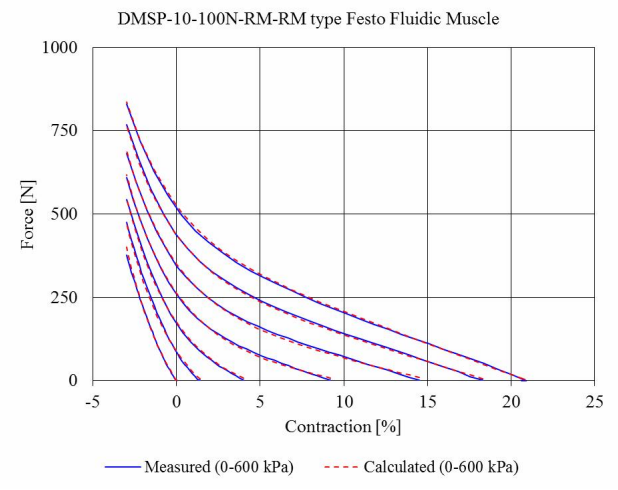

Figure 8
Comparison of measured and calculated force under different pressure values (0-600 kPa) using (3)

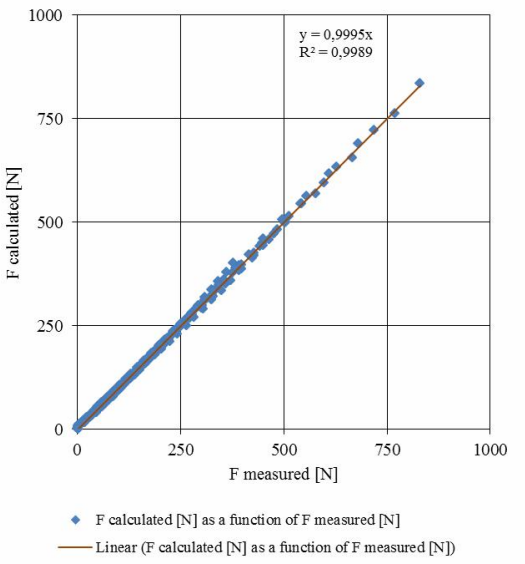

Figure 9
Result of regression and correlation analysis under different pressure values (0-600 kPa)

Next, the hysteresis in the force-length (contraction) loop was analysed. Fig. 10 illustrates the hysteresis loop under a pressure of 600 kPa, while Fig. 11 demonstrates it under different pressure values (0-600 kPa).

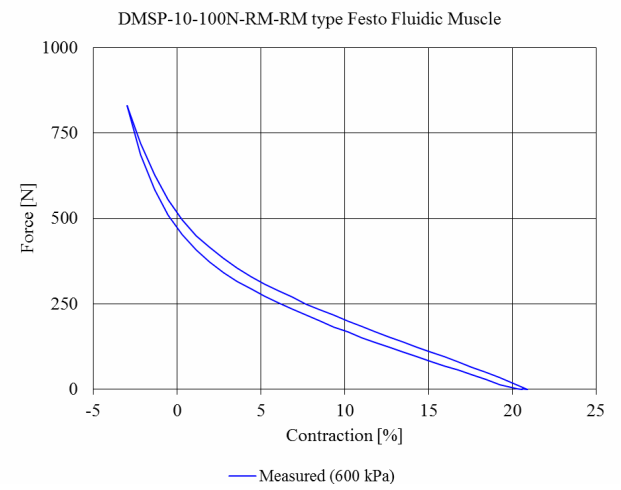

Figure 10
Hysteresis in the tension-contraction cycle under a pressure of 600 kPa

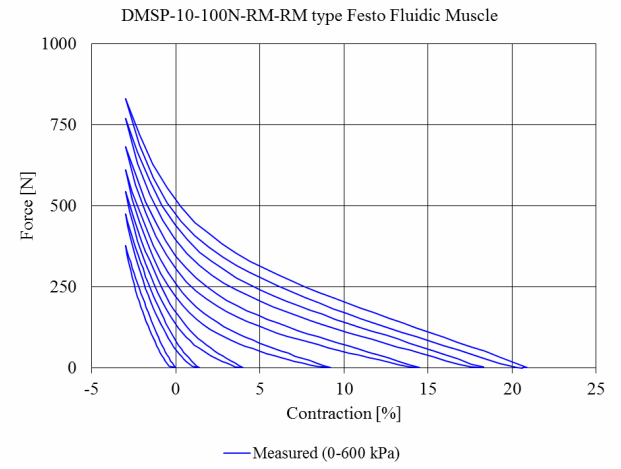

Figure 11
Hysteresis in the tension-contraction cycle under different pressure values (0-600 kPa)

To approximate the hysteresis loops using (3), besides the parameters in Table 1 and Table 2, new parameters had to be specified for lower curves (Table 3 and Table 4).

Table 3
Values of unknown parameters of (3) for lower curve (600 kPa)

Parameters	Values
a_1	-5.83
a_2	166.60
a_3	-0.40
a_4	-2.83
a_5	89.18
a_6	-193.56

Table 4
Values of unknown parameters of (3) for lower curves (0-600 kPa)

Parameters	Values
a_1	-6.45
a_2	166.51
a_3	-0.41
a_4	-2.88
a_5	89.89
a_6	-193.46

The accurate fitting of (3) for the hysteresis loops can be seen in Fig. 12 and Fig. 13. Finally, Fig. 14 and Fig. 15 prove the accuracy of static force model. Consequently, (3) is capable of making accurate and reliable predictions of static force.

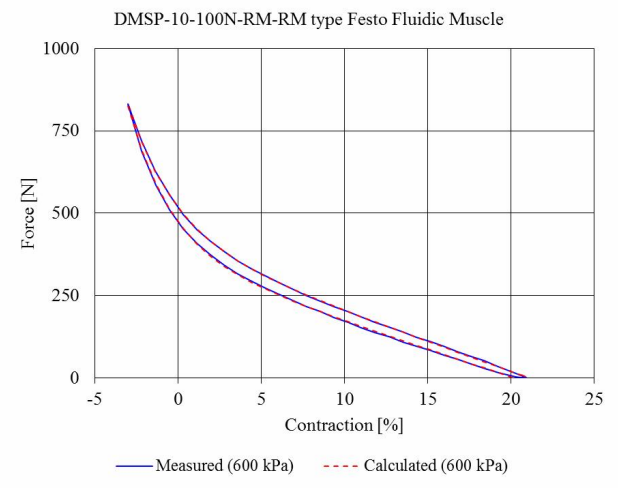

Figure 12
Approximation of hysteresis loop using (3) under a pressure of 600 kPa

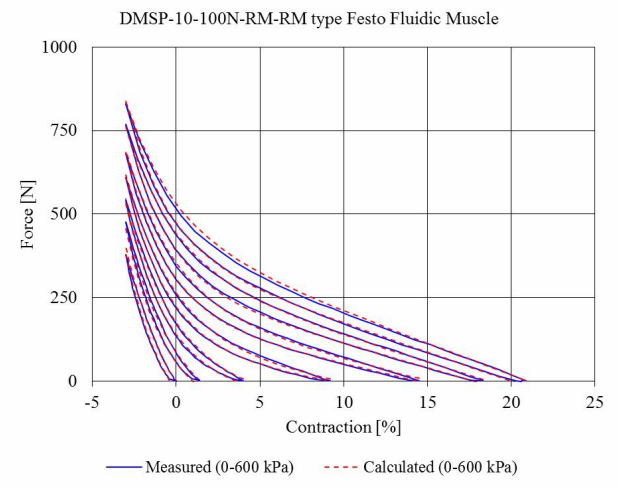

Figure 13
Approximation of hysteresis loops using (3) under different pressure values (0-600 kPa)

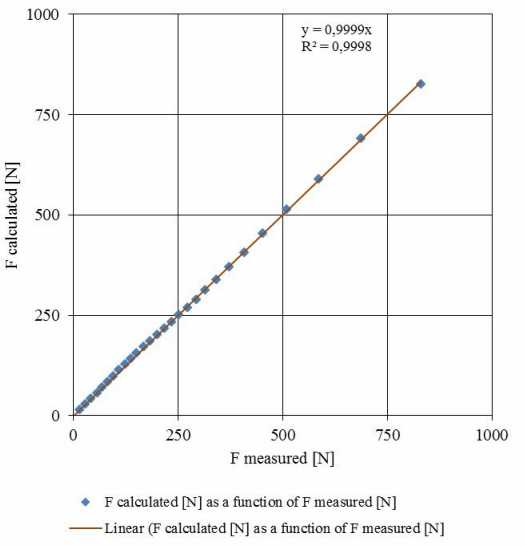

Figure 14
Result of regression and correlation analysis for lower curve under a pressure of 600 kPa

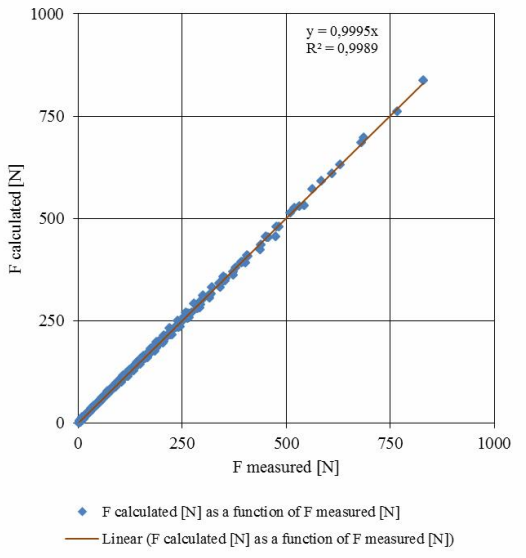

Figure 15
Result of regression and correlation analysis for lower curves under different pressure values (0-600 kPa)

Conclusions

This paper presents a static force model for Fluidic Muscles. It was proved that the six-parameter function can be used for accurate prediction of static force. The regression and correlation analysis were carried out in MS Excel environment. The behaviour of pneumatic artificial muscles under operation can be described by dynamic models. On the basis of this static force model a new dynamic model has been developed. With the help of dynamic model the stiffness and damping coefficient of PAMs can be determined and the whole system containing PAM can be described.

References

[1] D. G. Caldwell, A. Razak, M. J. Goodwin: Braided Pneumatic Muscle Actuators, IFAC Conference on Intelligent Autonomous Vehicles, Southampton, United Kingdom, 18-21 April, 1993, pp. 507-512.

[2] C. P. Chou, B. Hannaford: Measurement and Modeling of McKibben Pneumatic Artificial Muscles, IEEE Transactions on Robotics and Automation, 1996, Vol. 12, No. 1, pp. 90-102.

[3] F. Daerden: Conception and Realization of Pleated Artificial Muscles and Their Use as Compliant Actuation Elements, PhD Dissertation, Vrije Universiteit Brussel, Faculteit Toegepaste Wetenschappen Vakgroep Werktuigkunde, 1999, pp. 5-33.

[4] F. Daerden, D. Lefeber: Pneumatic Artificial Muscles: Actuator for Robotics and Automation, European Journal of Mechanical and Environmental Engineering, 2002, Vol. 47, pp. 10-21.

[5] B. Tondu, P. Lopez: Modeling and Control of McKibben Artificial Muscle Robot Actuator, IEEE Control System Magazine, 2000, Vol. 20, pp. 15-38.

[6] M. Balara, A. Petík: The Proporties of the Actuators with Pneumatic Artificial Muscles, Journal of Cybernetics and Informatics, 2004, Vol. 4, pp. 1-15.

[7] R. Ramasary, M. R. Juhari, M. R. Mamat, S. Yaacobs, N. F. Mohd Nasir, M. Sugisaka: An Application of Finite Modelling to Pneumatic Artificial Muscle, American Journal of Applied Sciences, 2005, Vol. 2, No. 11, pp. 1504-1508.

[8] Festo: Fluidic Muscle DMSP, with Press-fitted Connections, Fluidic Muscle MAS, with Screwed Connections, Festo Product Catalogue, 2005, p. 39

[9] K. Lamár, A. G. Kocsis: Implementation of Speed Measurement for Electrical Drives Equipped with Quadrature Encoder in LabVIEW FPGA, Acta Technica Corviniensis - Bulletin Of Engineering, 2013, Vol. 6. No.4, pp. 123-126.

[10] N. Yee, G. Coghill: Modelling of a Novel Rotary Pneumatic Muscle, Australiasian Conference on Robotics and Automation, Auckland, New Zealand, 27-29 November, 2002, pp. 186-190.

[11] T. Kerscher, J. Albiez, J. M. Zöllner, R. Dillmann: FLUMUT - Dynamic Modelling of Fluidic Muscles Using Quick-Release, 3rd International Symposium on Adaptive Motion in Animals and Machines, Ilmenau, Germany, 25-30 September, 2005, pp. 1-6.

[12] J. Borzikova, M. Balara, J. Pitel: The Mathematical Model of Contraction Characteristic $k = (F, p)$ of the Pneumatic Artificial Muscle, XXXII. Seminar ASR '2007 "Instruments and Control", Farana, Smutný, Kočí & Babiuch, Ostrava, 2007, pp. 21-25.

[13] J. Pitel, M. Tothova: Dynamic Modeling of PAM Based Actuator Using Modified Hill's Muscle Model, 14th International Carpathian Control Conference (ICCC), Rytro, Poland, 26-29 May, 2013, pp. 307-310.

[14] J. Sárosi, Z. Fabulya: New Function Approximation for the Force Generated by Fluidic Muscle, International Journal of Engineering, Annals of Faculty of Engineering Hunedoara, 2012, Vol. 10, No. 2, pp. 105-110.

[15] J. Sárosi, Z. Fabulya, G. Szabó, P. Szendrő: Investigations of Precise Function Approximation for the Force of Fluidic Muscle in MS Excel, Review of Faculty of Engineering (International Conference on Science and Technique in the Agri-Food Business, ICoSTAF 2012), 2012, Vol. 2012/3-4, pp. 1-8.